마이크로기공 고분자(PIM-1)의 분자량 분포에 따른 이산화탄소 기체 분리막의 성능 변화 연구

권 지 민 · 손 혜 정 · 김 진 욱 · 이 창 수[†]

국립부경대학교 화학공학과
(2023년 12월 5일 접수, 2023년 12월 6일 수정, 2023년 12월 6일 채택)

Effect of Molecular Weight Distribution of Intrinsically Microporous Polymer (PIM-1) Membrane on the CO_2 Separation Performance

Ji Min Kwon, Hye Jeong Son, Jin Uk Kim, and Chang Soo Lee[†]

Department of Chemical Engineering, Pukyong National University, Busan 48513, Republic of Korea

(Received December 5, 2023, Revised December 6, 2023, Accepted December 6, 2023)

요   약: 이 연구 논문은 기후 변화에 대한 전 세계적인 우려와 온실 가스 배출 감소를 위한 필수적인 요구에 대응하여 마이크로기공 고분자(PIM-1)의 이용을 탐구한 것이다. 연구는 PIM-1 막을 이산화탄소(CO_2) 가스 분리 막으로 사용하는 현대적인 소재로서의 응용에 집중하고 있다. 연구는 PIM-1 막의 합성, 분자량 제어, 그리고 제각각의 특성 분석 기술을 통해 포괄적인 통찰을 제공하며, 이러한 특성 분석 기술을 통해 PIM-1의 고유한 교차결합 및 강성 구조에서 비롯된 내재적 다공성이 특히 이산화탄소의 선택적 투과에 활용되고 있다. 논문은 PIM-1의 가교된 구조로부터 비롯된 내재적 다공성이 특히 이산화탄소의 선택적 투과에 활용되고 있다. 논문은 PIM-1의 튜닝 가능한 화학적 특성을 강조하며, 가스 분리 막의 맞춤 및 최적화를 가능케 하는 특성에 대한 이해를 제시하고 있다. 분자량을 통제함으로써 고분자량(H-PIM-1) 막은 낮은 분자량 대비 더 뛰어난 CO_2 투과성과 선택성을 나타내며, 이를 통해 PIM-1 막의 특성을 조절하는 데 분자량의 중요성을 강조하고 있다. 연구 결과는 PIM-1 막 특성을 조절하는 데 분자량이 중요한 역할을 하는 것을 강조하며, 이는 기후 변화의 긴급한 글로벌 도전에 대응하기 위한 효율적이고 선택적인 CO_2 포집을 위한 차세대 막 기술의 발전에 기여하고 있다.

Abstract: This research article explores the application of Polymer of Intrinsic Microporosity (PIM-1) as a cutting-edge material for CO_2 gas separation membranes in response to the escalating global concern over climate change and the imperative to reduce greenhouse gas emissions. The study delves into the synthesis, molecular weight control, and fabrication of PIM-1 membranes, providing comprehensive insights through various characterization techniques. The intrinsic microporosity of PIM-1, arising from its unique crosslinked and rigid structure, is harnessed for selective gas permeation, particularly of carbon dioxide. The article emphasizes the tunable chemical properties of PIM-1, allowing for customization and optimization of gas separation membranes. By controlling the molecular weight, higher molecular weight (H-PIM-1) membranes are demonstrated to exhibit superior CO_2 permeability and selectivity compared to lower molecular weight counterparts (L-PIM-1). The study's findings highlight the critical role of molecular weight in tailoring PIM-1 membrane properties, contributing to the advancement of next-generation membrane technologies for efficient and selective CO_2 capture —an essential step in addressing the pressing global challenge of climate change.

Keywords: CO_2 separation, membrane, polymer of intrinsic microporosity, molecular weight, permeability

1. Introduction

The escalating global concern over climate change and the imperative to reduce greenhouse gas emissions have intensified research efforts in developing innovative technologies for efficient carbon capture and

utilization. Among these, membrane-based gas separation has emerged as a promising avenue, offering a cost-effective and energy-efficient alternative to traditional separation methods. This paper delves into the forefront of this field, exploring the application of Polymer of Intrinsic Microporosity (PIM-1) as a cutting-edge material for CO_2 gas separation membranes[1-6].

PIM-1, renowned for its exceptional intrinsic microporosity, stands out as a polymer with unique structural characteristics that lend themselves well to gas separation applications. The intrinsic microporosity of PIM-1 arises from its highly crosslinked and rigid structure, which creates a network of micropores that selectively allows the permeation of certain gas molecules, such as carbon dioxide, while impeding others[7-9]. This inherent property positions PIM-1 as a promising candidate for enhancing the performance of gas separation membranes, particularly in the context of CO_2 capture from industrial processes and power plants.

The adoption of PIM-1 in gas separation membrane technology is not only driven by its inherent microporous structure but also by its tunable chemical properties[10-13]. Researchers have harnessed the versatility of PIM-1 to tailor its chemical composition, thereby fine-tuning its gas permeability and selectivity[14,15]. This level of customization enables the development of membranes optimized for specific gas separation tasks, making PIM-1 an invaluable tool in the quest for highly efficient and selective CO_2 capture.

In this paper, we aim to provide a comprehensive overview of recent advancements in the utilization of PIM-1 membranes for CO_2 gas separation. The molecular weight of PIM-1 was controlled by adjusting the synthesis condition such as temperature, chemical components and etc., to Fig. out the effect of backbone chain length on the CO_2 separation performance. By examining the synthesis methods, structural properties, and performance characteristics of these membranes, we seek to contribute to the growing body of knowledge that underpins the development of next-generation

membrane technologies with a focus on mitigating the impact of anthropogenic carbon emissions on the environment.

2. Materials and Methods

2.1. Materials

For the synthesis of PIM-1, 5,5',6,6'-Tetrahydroxy-3,3,3',3'-tetramethyl-1,1'-spirobisindane (TTSBI, 96%), tetrafluoroterephthalonitrile (TFTPN, 99%) and anhydrous potassium carbonate (K_2CO_3, 99.99%) were purchased from Sigma Aldrich, was sublimated under vacuum at room temperature before using. Anhydrous toluene (99.8%) and anhydrous N,N-dimethylacetamide (DMAc, 99.8%) from Sigma Aldrich were used as received. The above all chemicals were used without further purification.

2.2. Synthesis of PIM−1 using polycondensation method

TTSBI (10.0 mmol) and TFTPN (10.0 mmol) were combined in a solvent mixture of DMAc and toluene under N_2 atmosphere, with continuous stirring until complete dissolution was achieved. K_2CO_3 (6 g) was then introduced into the solution, and the mixture was stirred under N_2 for 1 hour. Subsequently, the reaction mixture underwent reflux under N_2 at 160°C for 4 hours, with simultaneous stirring. Upon completion of the reaction, the resulting polymer was precipitated in methanol to obtain the solid polymer form. The obtained polymer was redissolved in chloroform, followed by reprecipitation in methanol. After washing the polymer twice with hot deionized (D.I) water, solvent exchange was performed using methanol. The molecular weight was controlled with a different composition of solvent during the synthesis, such as the ratio between DMAc and toluene. The polymer was then dried at 60°C for 24 hours to achieve the final polymer product.

2.3. Fabrication of the PIM−1 membrane

The preparation of H-PIM-1 and L-PIM-1 membranes involved dissolving the polymers in chloroform

with vigorous stirring for 6 hours to achieve a 5 wt% solution. Subsequently, the polymer solution was cast onto a glass petri dish and covered directly with aluminum foil. The casting was left to dry at ambient temperature for 24 hours, followed by an additional 24 hours of vacuum oven drying. The resulting membranes were carefully peeled off from the glass dish, resulting in yellowish gas separation membranes. The thickness measurements indicated that H-PIM-1 and L-PIM-1 membranes had thicknesses of 187 μm and 193 μm, respectively.

2.4. Characterization

The morphology of membrane surface were observed using a field-emission scanning electron microscope-cold type (FE-SEM, JEOL, JSM6700F, 10 kV). The characterization bands of polymer were recorded using a Fourier transform-infrared spectroscopy (FT-IR, 300E, Shimadzu, Japan) in the attenuated total reflection (ATR) within wavenumber range of 4000-600 cm^{-1}. Number average molecular weight and polydispersity index (PDI) of PIM-1 were investigated via gel permeation chromatography (GPC, Shimadzu, Japan). The samples were dissolve in chloroform and tested at 30°C. The gas separation performance was measured *via* Time-lag method with the gas separation apparatus provided from the Airrrane Co. Ltd. using the CO_2 and N_2 pure gases. The ideal CO_2/N_2 selectivity was obtained by dividing the CO_2 permeability with N_2 permeability.

3. Results and Discussion

The synthesis process of intrinsically microporous polymer (PIM-1) is elucidated in Scheme 1, employing the polycondensation method[16]. The chemical structure of the PIM-1 backbone is intentionally designed to be bulky, disrupting molecular chain packing and facilitating the creation of a microporous architecture. The non-linear configuration of the polymer chains contributes to the formation of intrachain pores, establishing a highly permeable pathway for CO_2. This strategic molecular design enhances the overall gas separation performance of PIM-1, making it a promising candidate for applications requiring efficient gas permeation. The PIM-1 was then casted on the petri dish, followed by an evaporation of the solvents to obtain the free-standing PIM-1 membrane. The detailed explanation provided in Scheme 1 highlights the key structural features and synthesis principles crucial for the development of this intrinsically microporous polymer.

The chemical bonds in TFTPN, TTSBI, H-PIM-1, and L-PIM-1 were verified through FT-IR spectroscopy, as depicted in Fig. 1. The monomers displayed distinct vibrational modes corresponding to the aromatic C−H and C≡N bonds for TTSBI and TFTPN, respectively. Following polycondensation, the appearance of characteristic aromatic C=C bonds and C-H vi-
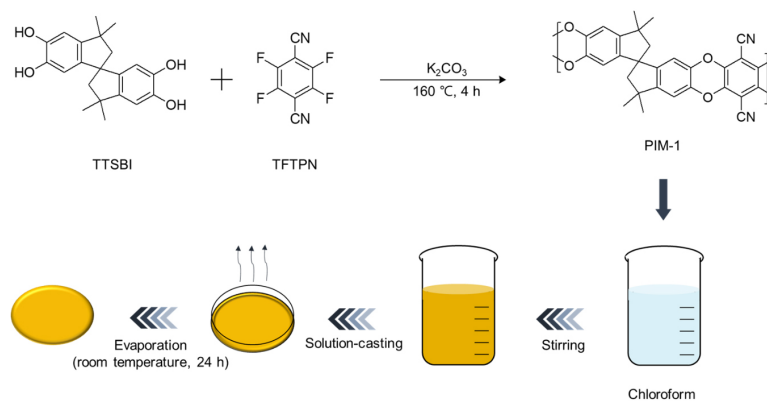
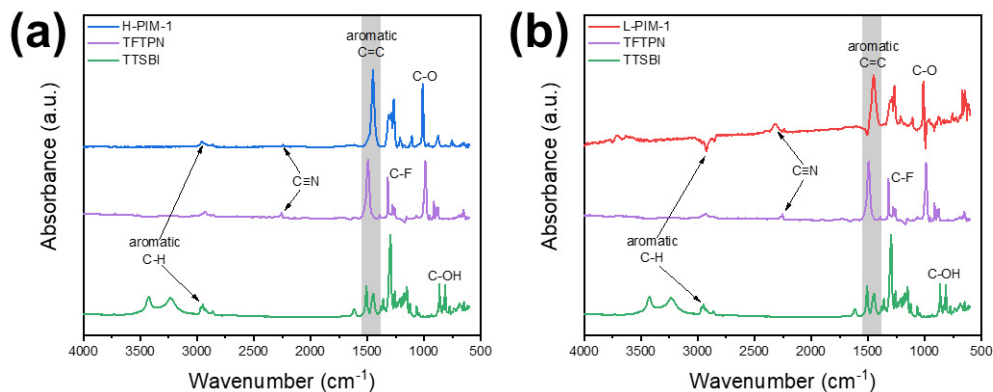**Scheme 1.** Schematic procedure to synthesize the PIM-1.

Fig. 1. FT-IR spectra of (a) H-PIM-1 and (b) L-PIM-1 compared with the respective monomers (TFTPN and TTSBI).

brational modes confirmed the presence of a bulky backbone in the PIM-1 chain. Notably, the $C-O$ stretching band of TFTPN (989 cm^{-1}) experienced a blue shift to a higher wavenumber (1013 cm^{-1}), indicating a significant increase in the strength of the $C-O$ bond, as predicted by Hooke's Law[17]:

$$\bar{\nu} = \frac{1}{2\pi c}\sqrt{\frac{k}{\mu}} \qquad (1)$$

where $\bar{\nu}$ is the wavenumber, k is the force constant, and μ is the reduced mass of the combined atoms. Furthermore, the characteristic bands of the aromatic $C-H$ bond in the PIM-1 backbone appeared at 2951 cm^{-1}, and the $C-F$ bond in TFTPN completely disappeared during the polycondensation process[18]. These observations provide conclusive evidence that PIM-1 was successfully synthesized, and the monomers were completely eliminated during the washing process.

GPC measurements were conducted to determine the molecular weights (MW) of H-PIM-1 and L-PIM-1. The molecular weight distribution, as indicated by retention time, revealed that H-PIM-1 eluted much faster than L-PIM-1. This disparity can be attributed to the pore penetration of L-PIM-1, providing a longer pathway for its elution. Consequently, it can be inferred that H-PIM-1 and L-PIM-1 were prepared with different molecular weights, with calculated values of 31,428 g mol^{-1} and 15,990 g mol^{-1}, respectively. The molecular
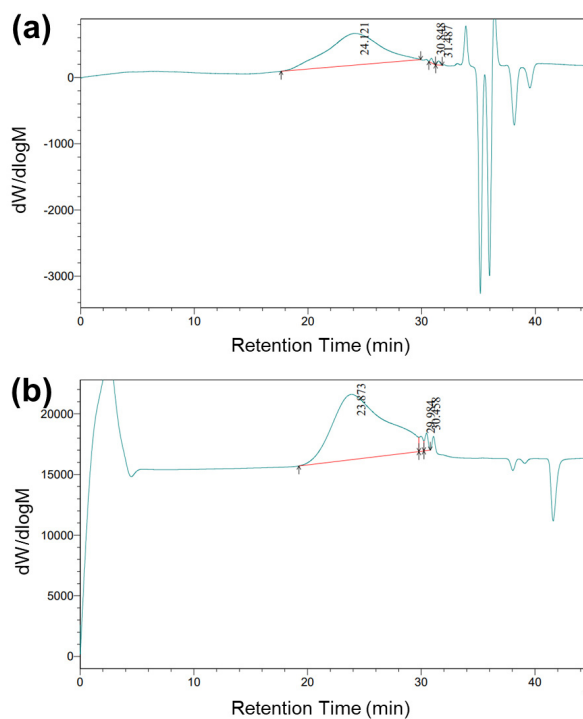

Fig. 2. GPC curves of (a) H-PIM-1 and (b) L-PIM-1.

weight of H-PIM-1 was nearly double that of L-PIM-1, presenting a significant variation. This distinction is crucial for evaluating the impact of molecular weight on the CO₂ separation performance of the membrane[19,20].

Fig. 3 presents FE-SEM images depicting the surfaces of H-PIM-1 and L-PIM-1 membranes, along with corresponding photographic images. In Fig. 3a, the surface of H-PIM-1 appears remarkably even, exhibiting
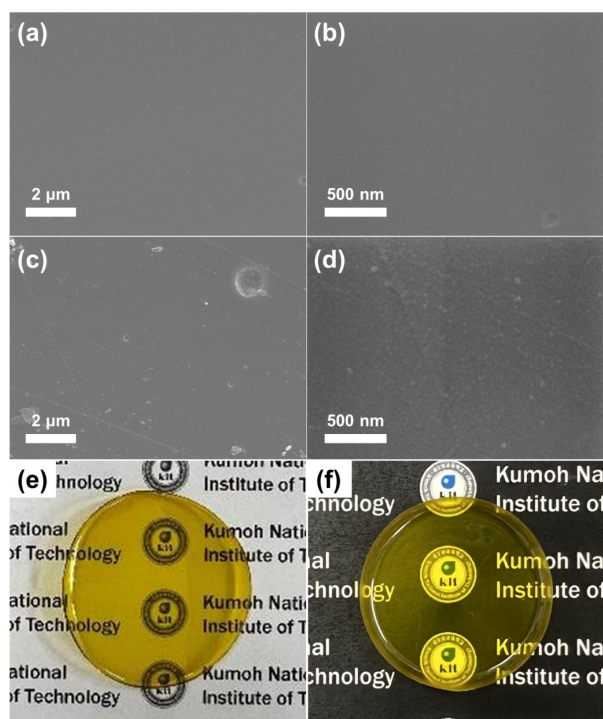
Fig. 3. FE-SEM surface images of (a, b) H-PIM-1 and (c, d) L-PIM-1 membrane and photographic images of (e) H-PIM-1 and (f) L-PIM-1 membranes.

Fig. 4. CO_2 and N_2 permeability and ideal CO_2/N_2 selectivity of H-PIM-1 and L-PIM-1 membrane calculated from the Time-lag method.

no significant cracks or bumpy morphology. Upon closer inspection in Fig. 3b, a slightly bumpy surface is observed, attributed to the bulky nature of the PIM-1 backbone, essential for constructing micropores. Conversely, Fig. 3c reveals that the L-PIM-1 membrane displays a rougher surface with pronounced bumps, indicative of its lower molecular weight designed to achieve membrane uniformity. Additionally, Fig. 3d illustrates a nanocrystal-like surface on L-PIM-1, highlighting a lack of physical properties conducive to forming a highly organized membrane[21]. Notably, the distinct colors of the membranes in Fig. 3e and f contribute further insights. H-PIM-1 exhibits a brownish hue, while L-PIM-1 appears more yellow. These visual differences align with the variations in molecular weight between H-PIM-1 and L-PIM-1, underscoring the influence of molecular weight on membrane properties.

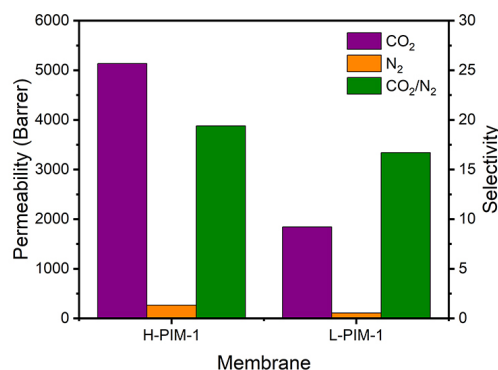Gas separation performance of H-PIM-1 and L-PIM-1 was investigated through the Time-lag method and described in Fig. 4. The H-PIM-1 achieved the CO_2 permeability of 5137 Barrer and CO_2/N_2 selectivity of 19.4 while the L-PIM-1 scored the CO_2 permeability of 1843 Barrer and CO_2/N_2 selectivity of 16.7. The higher permeability of H-PIM-1 would be attributed to the more developed microporous structure due to the higher chain length from the high MW, supported by the N_2 permeability which is highly affected by the diffusivity of membrane[22]. Moreover, the higher CO_2/N_2 selectivity was obtained in the H-PIM-1 membrane. This result is attributed to the more developed polar groups such as cyano group and ether group compared with those of L-PIM-1[23,24]. Therefore, the higher molecular weight from 15000 to 30000 g mol^{-1} resulted in the higher CO_2 separation performance. In this regard, the CO_2 separation membrane composed of polymer of intrinsic microporosity would be highly dependent on the molecular weight, which would provide a more CO_2-philic pathway and highway, simultaneously.

4. Conclusion

In conclusion, this study establishes Polymer of Intrinsic Microporosity (PIM-1) as a promising material for CO_2 gas separation membranes, emphasizing its unique structural characteristics and tunable chemical properties. The controlled synthesis of PIM-1, varying

its molecular weight, revealed a substantial influence on CO_2 separation performance. Higher molecular weight (H-PIM-1) membranes demonstrated superior CO_2 permeability and selectivity compared to lower molecular weight counterparts (L-PIM-1), attributed to a more developed microporous structure and enhanced polar groups. Comprehensive characterization, including FT-IR spectra, GPC curves, and FE-SEM images, provided insights into the membrane's composition, molecular weight distribution, and surface morphology. The study's findings underscore the critical role of molecular weight in tailoring PIM-1 membrane properties, contributing to the advancement of next-generation membrane technologies for efficient and selective CO_2 capture－a pivotal step towards mitigating anthropogenic carbon emissions and addressing the pressing global challenge of climate change.

Acknowledgements

Reference

1. Y. S. S. Young and P. Rajkumar, "Ionic liquid consisted of composite membrane for carbon dioxide separation: A review", *Membr. J.*, **33**, 240-247 (2023).

2. K. H. Chul, M.-J. Jeon, S.-C. Jung, and Y.-W. Jeon, "Preparation and properties of hollow fiber membrane for CO_2/H_2 separation", *Membr. J.*, **33**, 222-232 (2023).

3. X. Lv, X. Li, L. Huang, S. Ding, Y. Lv, and J. Zhang, "Tailoring physical and chemical microenvironments by polyether-amine in blended membranes for efficient CO_2 separation", *Korean J. Chem. Eng.*, **39**, 475-483 (2022).

4. S. He, B. Zhu, S. Li, Y. Zhang, X. Jiang, C. Hon Lau, and L. Shao, "Recent progress in PIM-1 based membranes for sustainable CO_2 separations: Polymer structure manipulation and mixed matrix membrane design", *Sep. Purif. Technol.*, **284**, 120277 (2022).

5. H. Iqubal, H. Asmaul, and P. H. Bum, "1,3-dioxolane-based CO_2 selective polymer membranes for gas separation", *Membr. J.*, **33**, 94-109 (2023).

6. S. Mohsenpour, A. W. Ameen, S. Leaper, C. Skuse, F. Almansour, P. M. Budd, and P. Gorgojo, "PIM-1 membranes containing POSS-graphene oxide for CO_2 separation", *Sep. Purif. Technol.*, **298**, 121447 (2022).

7. M. Tamaddondar, A. B. Foster, M. Carta, P. Gorgojo, N. B. McKeown, and P. M. Budd, "Mitigation of physical aging with mixed matrix membranes based on cross-linked PIM-1 fillers and PIM-1", *ACS Appl. Mater. Interfaces*, **12**, 46756-46766 (2020).

8. M. M. Khan, G. Bengtson, S. Shishatskiy, B. N. Gacal, M. M. Rahman, S. Neumann, V. Filiz, and V. Abetz, "Cross-linking of polymer of intrinsic microporosity (PIM-1) via nitrene reaction and its effect on gas transport property", *Eur. Polym. J.*, **49**, 4157-4166 (2013).

9. S. Thomas, I. Pinnau, N. Du, and M. D. Guiver, "Pure-and mixed-gas permeation properties of a microporous spirobisindane-based ladder polymer (PIM-1)", *J. Membr. Sci.*, **333**, 125-131 (2009).

10. M. Tian, S. Rochat, H. Fawcett, A. D. Burrows, C. R. Bowen, and T. J. Mays, "Chemical modification of the polymer of intrinsic microporosity PIM-1 for enhanced hydrogen storage", *Adsorption*, **26**, 1083-1091 (2020).

11. W. Han, C. Zhang, M. Zhao, F. Yang, Y. Yang, and Y. Weng, "Post-modification of PIM-1 and simultaneously in situ synthesis of porous polymer networks into PIM-1 matrix to enhance CO_2 separation performance", *J. Membr. Sci.*, **636**, 119544 (2021).

12. J. Jun Kyu, Y. Chaewon, and P. Ho Bum, "Surface modification of poly(tetrafluoroethylene) (PTFE) membranes", *Membr. J.*, **33**, 1-12 (2023).

13. R. Swaidan, B. S. Ghanem, E. Litwiller, and I. Pinnau, "Pure-and mixed-gas CO_2/CH_4 separation

properties of PIM-1 and an amidoxime-functional-ized PIM-1", *J. Membr. Sci.*, **457**, 95-102 (2014).

14. J. Guan, X. Wang, J. Du, Q. Liang, W. He, Y. Liu, J. Ma, C. Zhang, and J. Liu, "Surface-engineered PIM-1 membranes for facile CO_2 capture", *Chem. Eng. J.*, **477**, 147017 (2023).

15. X. Niu, G. Dong, D. Li, Y. Zhang, and Y. Zhang, "Atomic layer deposition modified PIM-1 membranes for improved CO_2 separation: A comparative study on the microstructure-performance relationships", *J. Membr. Sci.*, **664**, 121103 (2022).

16. P. M. Budd, B. S. Ghanem, S. Makhseed, N. B. McKeown, K. J. Msayib, and C. E. Tattershall, "Polymers of intrinsic microporosity (PIMs): Robust, solution-processable, organic nanoporous materials", *Chem. Commun.*, **2**, 230-231 (2004).

17. J. T. Burke, "IR spectroscopy or Hooke's law at the molecular level-a joint freshman physics-chemistry experience", *J. Chem. Educ.*, **74**, 1213 (1997).

18. F. Y. Li, Y. Xiao, T.-S. Chung, and S. Kawi, "High-performance thermally self-cross-linked polymer of intrinsic microporosity (PIM-1) membranes for energy development", *Macromolecules*, **45**, 1427-1437 (2012).

19. I. Ponomarev, D. Y. Razorenov, I. Blagodatskikh, A. Muranov, L. Starannikova, A. Y. Alent'ev, R. Y. Nikiforov, and Y. P. Yampol'skii, "Polymer with intrinsic microporosity PIM-1: New methods of synthesis and gas transport properties", *Polym. Sci. Ser. B*, **61**, 605-612 (2019).

20. R. Hou, S. J. Smith, C. D. Wood, R. J. Mulder, C. H. Lau, H. Wang, and M. R. Hill, "Solvation effects on the permeation and aging performance of PIM-1-based MMMs for gas separation", *ACS Appl. Mater. Interfaces*, **11**, 6502-6511 (2019).

21. J. Li, M. Zhang, W. Feng, L. Zhu, and L. Zhang, "PIM-1 pore-filled thin film composite membranes for tunable organic solvent nanofiltration", *J. Membr. Sci.*, **601**, 117951 (2020).

22. H. W. Kim, "Intrinsic permeation properties of graphene oxide membranes for gas and ion separations", *Membr. J.*, **32**, 1-12 (2022).

23. E. S. Yi, S. R. Hong, and H. K. Lee, "CO_2 separation performance of PEBAX mixed matrix membrane using PEI-GO@ZIF-8 as filler", *Membr. J.*, **33**, 23-33 (2023).

24. W. Fan, S. Yuan, W. Wang, L. Feng, X. Liu, X. Zhang, X. Wang, Z. Kang, F. Dai, and D. Yuan, "Optimizing multivariate metal−organic frameworks for efficient C_2H_2/CO_2 separation", *J. Am. Chem. Soc.*, **142**, 8728-8737 (2020).